Measurement of Nucleon Structure Function in Muon Scattering at High q^2

R. C. Ball, D. Bauer, C. Chang,[a] K. W. Chen, S. Hansen,[b] J. Kiley, I. Kostoulas,[b] A. Kotlewski,[c] L. Litt,[c] and P. F. Schewe[d]
Michigan State University, East Lansing, Michigan 48824

and

A. Van Ginneken
Fermi National Accelerator Laboratory, Batavia, Illinois 60510
(Received 26 December 1978)

The nucleon structure function, F_2, has been measured up to $q^2 = 120$ (GeV/c)^2 and for $40 < W^2 < 300$ GeV^2. The data exhibit a significant pattern of scaling violation. Compared to lower-energy data, F_2 shows an observable increase of ~15% at high q^2 for $x < 0.4$. The pattern of the increase may accommodate a threshold in W or new theoretical parametrizations.

Previous experiments[1-3] on deep-inelastic muon and electron scattering have established significant deviations from Bjorken scaling[4] up to $q^2 = 50$ (GeV/c)^2. The nucleon structure function, $F_2(x, q^2)$, can no longer be expressed as a function of a single scaling variable, say x ($\equiv q^2/2M\nu$, where q^2 is the square of the four-momentum transfer of the scattered muon, M is the nucleon mass, and $\nu \equiv E_0 - E'$ is the difference in energy of incident and scattered μ). Theoretical interpretations[5] of nonscaling behavior include field-theoretic arguments, composite constituents of the nucleon, gauge theory of strong interactions with color degree of freedom [quantum chromodynamics (QCD)], and new hadronic degrees of freedom in deep inelastic processes.

The present experiment, carried out at Fermilab, increases significantly the statistical certainty and the kinematical range over which deep-inelastic muon scattering ($\mu N \to \mu X$) has thus far been explored. For 2×10^{10} incident muons with an energy of 270 GeV (μ^+ and μ^-), 10^6 deep inelastic events above $q^2 = 5$ (GeV/c)^2 are recorded. Results from a large fraction of the μ^+ exposure are reported. The target consisted of a 7.4-m-long (4260-g/cm^2) iron-scintillator calorimeter which also measured the final-state hadron energy. Following the target was a 745-g/cm^2-thick steel hadron shield and a spectrometer[6] consisting of eight toroidal magnets (4973 g/cm^2 thick and about 90 cm in radius). Both the hadron shield and spectrometer were interleaved with wire spark chambers. In addition, three vertical and horizontal trigger bands of scintillation counters were positioned within the spectrometer. Three scintillation counters (15.9 cm radius) centered on the beam axis formed a veto which eliminated events with a penetrating particle at a small angle. Proportional chambers and beam halo veto (scintillation) counters defined the incident muon.

The momentum of the scattered muon is determined from its trajectory through the magnetic spectrometer. Track-finding efficiencies vary from 80% at low q^2 to 90% at high q^2 ($\gtrsim 50$ GeV^2/c^2). The resolution of the spectrometer was about 9%, with its central value calibrated to about 0.7%. The scattering angle is known to 0.4 mrad. The energy of the incident muon is determined to within 0.75%. The apparatus acceptance was relatively large (>50%) for events having a scattered muon energy $E' > 50$ GeV and an angle $20 < \theta < 80$ mrad. Figure 1 shows curves of equal apparatus acceptance in the q^2-ν plane. Also shown are lines of constant W^2 ($\equiv 2M\nu - q^2 + M^2$), the square of the center-of-mass energy of the virtual-photon–nucleon system. To reduce acceptance uncertainties, minimum scattering angle (10 mrad) and radius cuts (15.3 cm) were ap-

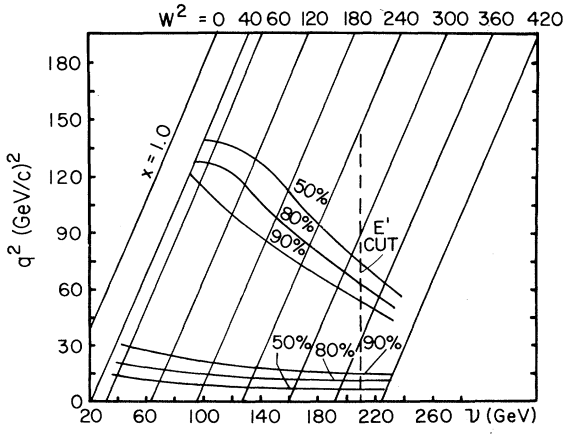

FIG. 1. Contour plot of apparatus acceptance as a function of q^2 and ν. Also shown are lines of constant W^2.

plied so as to accept only those muon tracks in the higher-acceptance regions away from the central hole (1.1×10^5 events).

The values of the structure function, F_2 per nucleon, were obtained from comparing the data to Monte Carlo predictions based on fits[7] of lower-energy data in F_2^{ep} and F_2^{ed} and, with nearly the same result, using a QCD parametrization.[8] The calculation included effects of real incident beam distributions, Fermi motion of the nucleons in the iron nucleus, radiative corrections, and wide-angle bremsstrahlung in simulating deep inelastic scattering. Incident and scattered muons are traced through the apparatus undergoing simulated magnetic deflection, multiple Coulomb scattering, μ-e scattering, bremsstrahlung, and collision losses. Further analysis treats data and Monte Carlo events identically. The data presented below show only statistical errors and do not include relative systematic and normalization uncertainties estimated to be about 10%. To arrive at the final overall normalization, corrections were applied to account for track-reconstruction inefficiencies (3%), hardware failure (2%), and effect on the muon flux due to trigger inefficiencies (7%). Uncertainties in these corrections do not influence the q^2 dependence observed in this experiment.

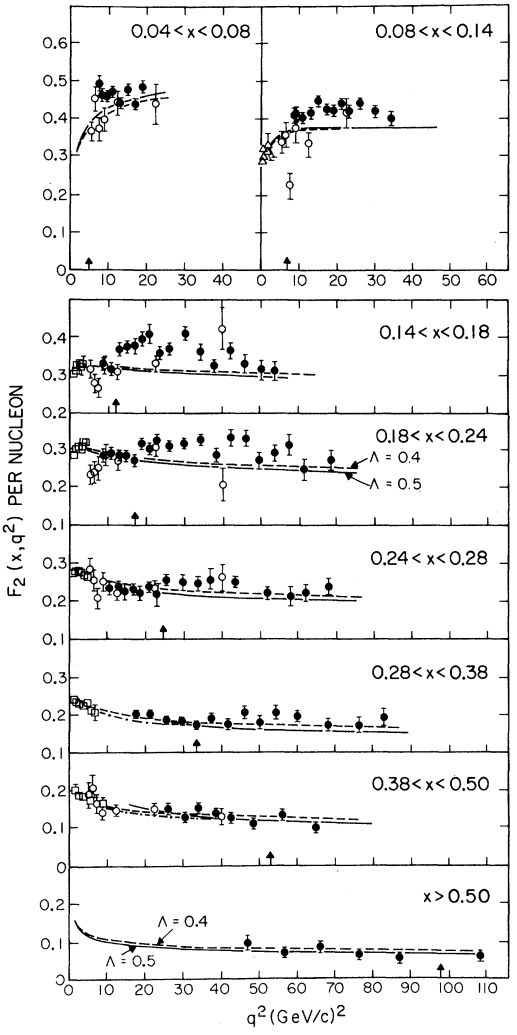

FIG. 2. Nucleon structure function F_2 vs q^2 for eight bands of x. Shown also are $F_2^{ed}/2$ (open square) of Ref. 3, and $F_2^{\mu p}$ of Ref. 2 (open circle) corrected for n-p differences. The solid, dashed, and dash-dotted lines are QCD predictions as explained in the text. The value $W^2=80$ GeV^2 is indicated by arrows. Errors are statistical.

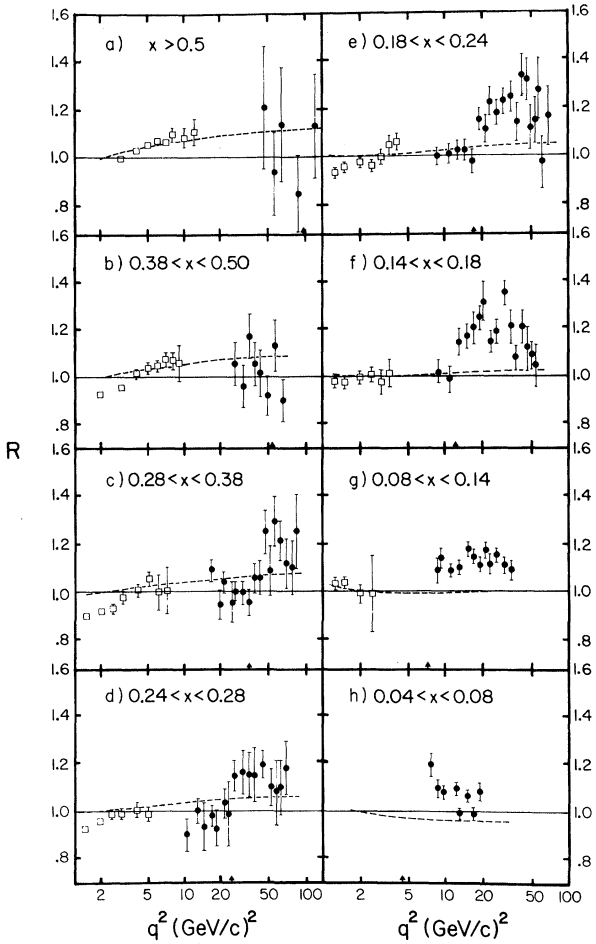

FIG. 3. Ratio of the observed to calculated (QCD) structure function ($\Lambda=0.5$ GeV) vs q^2 for eight bands of x. The value $W^2=80$ GeV^2 is indicated by arrows. The dashed line is the ratio of the QCD prediction for $\Lambda=0.4$ to that for $\Lambda=0.5$ GeV/c. Open squares show ratio for F_2^{ed}.

Figure 2 shows $F_2(\bar{x}_i, q^2)$ vs q^2 for successive x regions, where $\bar{x}_i$ is the weighted average of x for the ith data point. Also shown are QCD predictions[8] both for $F_2(\bar{x}_i, q^2)$ (the solid curve $\Lambda = 0.5$) and for $F_2(\bar{x}, q^2)$ (the dash-dotted curve, $\Lambda = 0.5$, dashed curve, $\Lambda = 0.4$), where $\bar{x}$ is the weighted average value for the entire x region. For lower x regions (<0.4), the data show a consistent pattern of near agreement with QCD at low q^2 and a tendency to rise above QCD at higher q^2. Note that in the region of overlap, the data agree with the other $F_2^{\mu p}$ results[2] to within 10%, giving our data an independent check on normalization uncertainties. In Figs. 3(a)–3(h), the ratio R $[\equiv F_2(\bar{x}_i, q^2)/F_2(\bar{x}_i, q^2)_{\mathrm{QCD}}]$ is plotted versus $\ln q^2$ for successive x cuts. The values of R for the data of Riordan *et al.*,[3] calculated in a similar manner, are also shown. The ratio of the QCD prediction for $\Lambda = 0.5$ GeV/c is shown as a dashed line. In Figs. 3(c)–3(f), where the data disagree with the QCD prediction, the difference due to this change of Λ is not significant. This behavior of F_2 vs q^2 at a fixed x is statistically consistent with that expected from a threshold behavior in the variable W^2.

In Fig. 4, R is plotted against W^2 for all q^2 and x. Beyond $W^2 = 80 \pm 10$ GeV^2, $R(W^2)$ is consistent with a rise of 12–15% above the lower-W^2 data. Table I shows sample tests of a possible W^2-threshold behavior. The data are fitted by (a) a straight line, (b) two separate straight lines on either side of $W^2 = 80$, and (c) two separate constants. Both (b) and (c) are favored over (a). A QCD prediction[8] is also tested.

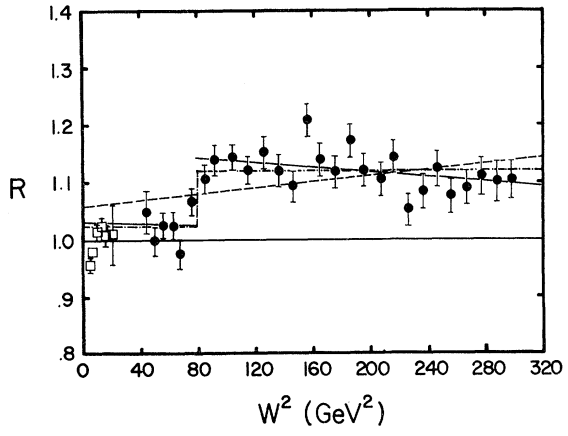

FIG. 4. R, ratio of observed-to-calculated (QCD) structure function vs W^2, for all q^2 and x. Shown are fits to (a) $R = a(W^2) + b$ (dashed line), (b) separate lines for the range $80 < W^2$ and $W^2 < 80$ GeV^2 (solid lines), and (c) two separate constants (dash-dotted line). $F_2^{\mathrm{el}}/2$ data [$q^2 > 2.0$ (GeV/c)^2] (Ref. 3) are shown (open square) but not fitted. Errors are statistical.

This observed behavior of F_2 in q^2 or W^2 cannot be accounted for by known systematic effects which include uncertainties in measurement of E_0, E', and θ, variation[9] in σ_s/σ_T or in the application of radiative corrections, and corrections for wide-angle bremsstrahlung and Fermi motion. The apparatus acceptance is a smooth function in W^2 and cannot accommodate a point-to-point rapid variation of F_2 in the range $65 < W^2 < 95$ GeV^2. For $x > 0.2$, variation in acceptance is less than 10% over this W^2 interval, with the variation decreasing as x increases. The effect of this variation has been taken into account in the analysis. We note, for example, in Fig. 3(c) the acceptance is greater than 80% for the entire set, and greater than 90% at the indicated arrow. The average scattering angles, $\langle\theta\rangle$, in Figs. 3(c)–3(e) are 16, 19, and 24 mrad, well above the minimum angle of 10 mrad. Although $F_2(x, q^2)$ can conceivably be more closely fitted by readjustments of q_0^2, Λ, quark, or gluon distributions in QCD, the observed q^2 or W^2 variation is not easily accommodated without major new assumptions since $F_2(q^2)|_x$ should be monotonic in q^2 or W^2, in contrast to the observed trend in this experiment.[10]

We acknowledge the support of the staff of Fermilab. We thank K. Thorne and M. Ghods for their help in data reduction. One of us (K.W.C.) would like to thank E. Lehman for useful discussions. This research was supported in part by the National Science Foundation under Grant No. 60950 and by the U. S. Department of Energy under Contract No. E(11-1)-1764.

TABLE I. Fits to $R = a(W^2) + b$. The χ^2 per degree of freedom are given in the last column.

W^2 region	a ($\times 10^4$)	b	χ^2/d.f.
All W^2	2.64 ±0.66	1.058 ±0.011	96.3/27
$W^2 < 80$[a]	−0.72 ±9.52	1.030 ±0.058	11.3/5
$W^2 > 80$	−2.11 ±0.91	1.159 ±0.017	25.8/20
All W^2	0[b]	1.097 ±0.005	112.4/28
$W^2 < 80$[a]	0[b]	1.025 ±0.010	11.3/6
$W^2 > 80$	0[b]	1.121 ±0.006	31.2/21
All W^2	0[b]	1.00[c]	485.4/29

[a]The choice of $W^2 = 80$ GeV^2 is dictated by the best possible fit. χ^2/d.f. improves further when resolution effects are included.

[b]The slope is set to zero, i.e., R = const.

[c]Ratio of measured F_2 to QCD prediction of Ref. 8.

Note added.—We have received a preprint on the experiment of de Groot *et al.*[11] After taking account of the variations of F_2^{ν} due to $\langle x \rangle$ in the larger Δx (=0.1) bins, normalization uncertainties, varying data-point density, and possible uncertainties in the 18/5 multiplier as a constraint to the data (especially at large W^2), we cannot infer any significant agreement (or disagreement) between F_2^{ν} and F_2^{μ} as presented here.

[a] Present address: National Central University, Chung-Li, Taiwan, Republic of China.
[b] Present address: Fermi National Accelerator Laboratory, Batavia, Ill. 60510.
[c] Present address: University of Miami School of Medicine, Biscayne Annex, Miami, Fla. 33152.
[d] Present address: Brookhaven National Laboratory, Upton, N. Y. 11973.

[1] C. Chang *et al.*, Phys. Rev. Lett. 35, 901 (1975).
[2] H. L. Anderson *et al.*, Phys. Rev. Lett. 38, 1450 (1976), and 41, 615 (1978).
[3] E. M. Riordan *et al.*, SLAC Report No. SLAC-PUB-1634, 1975 (unpublished).
[4] J. D. Bjorken, Phys. Rev. 179, 1547 (1969).
[5] E.g., H. Cheng and T. T. Wu, Phys. Rev. Lett. 22, 1409 (1969); K. Matsumoto, Prog. Theor. Phys. 47, 1975 (1972); M. S. Chanowitz and S. D. Drell, Phys. Rev. Lett. 30, 1975 (1973); H. D. Politzer, Phys. Rep. 14c, 129 (1974) and references therein; M. Y. Han and Y. Nambu, Phys. Rev. 139, B1006 (1965); J. C. Pati and A. Salam, Phys. Rev. Lett. 36, 11 (1976).
[6] K. W. Chen, in *Proceedings of the International Symposium on Lepton and Photon Interactions at High Energies, Hamburg, 1977*, edited by F. Gutbrod (DESY, Hamburg, Germany, 1977), p. 467.
[7] S. Stein *et al.*, Phys. Rev. D 12, 1884 (1975).
[8] A. Buras and B. G. F. Gaemers, to be published, and private communication. The parton distributions for the proton with a scale parameter $\Lambda = 0.5$ GeV/c at $q_0^2 = 2$ (GeV/c)^2 are $xS = (1-x)^8$, $xG = 2.41(1-x)^5$, $xC = 0$, $xu_v = 3/B(0.7, 3.6)x^{0.7}(1-x)^{2.6}$, and $xd_v = 1/B(0.85, 4.35)x^{0.85} \times (1-x)^{3.35}$. For the neutron, u_v and d_v distributions are interchanged. $\Lambda = 0.5$ GeV/c is preferred by recent fits to lepton scattering data.
[9] F_2 is extracted assuming R ($\equiv \sigma_S/\sigma_T$) = 0.25. By assuming $R = 0.44$, the variation of the cross section is less than 2% for the range of the data presented here.
[10] In QCD, the moment integrals $M_n(q^2) = \int_0^1 dx\, x^n [F_2(x, q^2)]$ vary as $a_n/(\ln q^2 \Lambda^2)^{b_m}$, where a_n, b_n, and Λ are constants. For a fixed x, $\partial F_2(x, q^2)/\partial \ln q^2$ is constant. Thus $F_2(q^2)$ varies montonically in q^2.
[11] J. G. H. de Groot *et al.*, "Inclusive Charged Current Interactions of High Energy Neutrinos and Antineutrinos in Iron" (to be published).

What Makes νW_2 Rise?

Elliot Lehman
Department of Physics, Michigan State University, East Lansing, Michigan 48824
(Received 27 September 1978)

Various models for the recently observed rise in $\nu W_2(x, Q^2)$ in deep-inelastic muon-Fe scattering at large Q^2 are considered. Explicit excitation of color seems to give the best fit to the data. Some consequences of this idea are discussed and predictions made to test it.

An unexpected rise in the deep-inelastic structure function of the nucleon has been reported.[1] (See also Riordan *et al.*[2] for older data.) This rise occurs at a fixed threshold in the virtual-photon–nucleon invariant mass of $W^2 = 80 \pm 10$ GeV$^2/c^2 \equiv W_{\text{thres}}^2$. Its position is independent of $x = Q^2/2m\nu$ (and, thus, $\omega = 1/x$). The expected behavior of $\nu W_2(x, Q^2)$ is quite different in, say, quantum chromodynamics (QCD).[3] The induced radiation of chargeless gluons reduces the momentum fraction of the charged quarks and $\nu W_2(x, Q^2)$ is a decreasing function of Q^2 for $x > 0.1$–0.2 and an increasing function at $x < 0.1$–0.2. The QCD results of Buras[3] for isoscalar νW_2 which give a good fit to the data of Ref. 1 (which uses an iron target) for $W^2 < W_{\text{thres}}^2$, fall well below the experimental points at larger W^2 (see Fig. 1). With the nucleon mass equal to m,

$$W^2 = 2m\nu - Q^2 + m^2, \tag{1}$$

so that $W^2 \geq W_{\text{thres}}^2$ at fixed x corresponds to

$$Q^2 > Q_{\text{thres}}^2(x) = (W_{\text{thres}}^2 - m^2)x/(1-x)$$
$$= (W_{\text{thres}}^2 - m^2)/(\omega - 1). \tag{2}$$

Thus the rise of $\nu W_2(x, Q^2)$ above the QCD prediction occurs for $Q^2 > Q_{\text{thres}}^2(x)$.

Reference 1 exhibits two different QCD fits to their data; both are inadequate when $W^2 > W_{\text{thres}}^2$. It is possible to force νW_2 to rise by taking a low-momentum-transfer boundary for perturbation theory at $Q^2 = 11$ GeV$^2/c^2$. However, the shape of